

# A Green Synthesis Strategy for Cobalt Phosphide Deposited on N, P Co-Doped Graphene for Efficient Hydrogen Evolution

Jingwen Ma <sup>1,\*</sup>, Jun Wang <sup>2</sup>, Junbin Li <sup>1</sup>, Ying Tian <sup>1</sup> and Tianai Zhang <sup>1</sup>

<sup>1</sup> School of Chemical and Environmental Engineering, China University of Mining and Technology (Beijing), Beijing 100083, China; lijunbin3293@163.com (J.L.); hlj5250@126.com (Y.T.); zta5540@163.com (T.Z.)

<sup>2</sup> PetroChina Planning and Engineering Institute, Beijing 100083, China; wangjun87@petrochina.com.cn

\* Correspondence: jingwen-ma@cumtb.edu.cn

**Abstract:** The exploitation of electrocatalysts with high activity and durability for the hydrogen evolution reaction is significant but also challenging for future energy systems. Transition metal phosphides (TMPs) have attracted a lot of attention due to their effective activity for the hydrogen evolution reaction, but the complicated preparation of metal phosphides remains a bottleneck. In this study, a green fabrication method is designed and proposed to construct N, P co-doped graphene (NPG)-supported cobalt phosphide (Co<sub>2</sub>P) nanoparticles by using DNA as both N and P sources. Thanks to the synergistic effect of NPG and Co<sub>2</sub>P, the Co<sub>2</sub>P/NPG shows effective activity with a small overpotential of 144 mV and a low Tafel slope of 72 mV dec<sup>-1</sup> for the hydrogen evolution reaction. This study describes a successful green synthesis strategy for the preparation of high-performance TMPs.

**Keywords:** cobalt phosphide; hydrogen evolution reaction; DNA; phosphorus source

## 1. Introduction

Hydrogen energy is regarded as the disruptive technological direction of the future energy revolution. The hydrogen energy industry is now essential to the national energy strategies of many countries. The question of how to obtain hydrogen in a large, cheap, convenient, and green way is the primary problem facing the development of hydrogen energy. Water electrolysis is considered to be a promising direction for future hydrogen production, especially electrolyzing water through using renewable energy and abandoned electricity [1–3]. Highly efficient catalysts are crucial for reducing the energy barrier for the hydrogen evolution reaction (HER). It is well-known that, at present, platinum-based catalysts are the most effective catalysts for the HER. However, their commercial application is restricted by their expensive cost and insufficient supply. Therefore, the development of non-noble metal-based electrocatalysts with high activity and stability is urgent for practical applications.

Recently, various non-noble metal electrocatalysts, such as transition metal sulfides [4,5], nitrides [6], and phosphides [7], have been developed for the hydrogen evolution reaction. Among them, transition metal phosphides have attracted a lot of attention due to abundant reserves and superior catalytic performance in the hydrogen evolution reaction [8–10]. Due to the various forms of cobalt phosphides, such as CoP, Co<sub>2</sub>P, CoP<sub>2</sub>, CoP<sub>3</sub>, etc., the reported synthesis methods are relatively limited. Meanwhile, the commonly used method for synthesizing phosphides is the gas–solid strategy, and the main precursor of the phosphorus used is sodium hypophosphite, which may release highly toxic phosphine (PH<sub>3</sub>) [11,12]. Graphene has an extremely large specific surface area and excellent conductivity, making it a rational carrier for hydrogen evolution catalysts [13–15]. In recent years, it has been found that doped graphene can activate adjacent carbon atoms to promote hydrogen evolution due to the difference in electronegativity and size between the doped heteroatoms and carbon atoms. Qiao et al. [16] obtained N, Co co-doped graphene by using melamine as a nitrogen source and triphenylphosphine as a phosphorus source and calcining it in an argon



**Citation:** Ma, J.; Wang, J.; Li, J.; Tian, Y.; Zhang, T. A Green Synthesis Strategy for Cobalt Phosphide Deposited on N, P Co-Doped Graphene for Efficient Hydrogen Evolution. *Materials* **2023**, *16*, 6119. <https://doi.org/10.3390/ma16186119>

Academic Editor: Federica Bianco

Received: 30 June 2023

Revised: 24 July 2023

Accepted: 25 July 2023

Published: 7 September 2023



**Copyright:** © 2023 by the authors. Licensee MDPI, Basel, Switzerland. This article is an open access article distributed under the terms and conditions of the Creative Commons Attribution (CC BY) license (<https://creativecommons.org/licenses/by/4.0/>).

atmosphere. Nitrogen and phosphorus heteroatoms affect the valence orbital energy levels of graphene, resulting in better catalytic activity for the hydrogen evolution by affecting nearby carbon atoms on the inactive graphene. The reaction steps for the preparation of metal phosphides and N, P co-doped graphene are generally complicated and usually include a high-temperature carbonization and a phosphating process. Therefore, it is necessary to find a simple and feasible method that can obtain NPG and directly synthesize cobalt phosphide at the same time to simplify the reaction. Deoxyribonucleic acid (DNA) is a biomolecule composed of four types of deoxyribonucleotides. Deoxyribonucleotides generally consist of one molecule of a nitrogenous base, one molecule of deoxyribose, and one molecule of phosphate [17]. From their composition, they can provide nitrogen and phosphorus for composite materials [18,19].

In this study, we describe the synthesis of a N, P co-doped graphene-supported cobalt phosphide composite (Co<sub>2</sub>P/NPG), which was synthesized through a hydrothermal reaction and a subsequent carbonization process. The biomolecule DNA was the nitrogen and phosphorus source for the preparation of NPG and Co<sub>2</sub>P, also acting as the chelating sites for metal ions. The as-prepared Co<sub>2</sub>P/NPG shows superior activity for the hydrogen evolution reaction.

## 2. Materials and Methods

**Preparation of Co<sub>2</sub>P/NPG:** First, graphene oxide (GO) was prepared using Hummers' method. For this, 20 mg GO and 30 mL deionized water were added into a 100 mL flask; this was followed by ultrasonication for 30 min to obtain a dilute solution of GO. Then, 100 mg deoxyribonucleic acid (DNA) was added to the GO solution, and the mixture was ultrasonicated for two hours to obtain a uniformly dispersed solution. Then, the above-mentioned mixture was heated to 95 °C in an oil bath and maintained for 30 min via magnetic stirring to obtain DNA-modified GO (DNA-GO). A total of 100 mg cobalt acetate hexahydrate was dissolved in the DNA-GO solution, and 0.25 mL ammonia solution was added drop by drop into the above-mentioned mixture. After continuous magnetic stirring for 3 h, the solution was transferred into a stainless-steel reactor and maintained at 180 °C in a vacuum drying oven for 3 h. The intermediate product (Co<sub>3</sub>O<sub>4</sub>/DNA-GO) was obtained after being centrifuged and washed several times. Finally, the Co<sub>3</sub>O<sub>4</sub>/DNA-GO was placed in a quartz boat in a tubular furnace and heated to 800 °C at a heating rate of 5 °C min<sup>-1</sup> in an Ar atmosphere before being kept for 2 h. After washing and filtering with deionized water, the Co<sub>2</sub>P/NPG composite was obtained by vacuum drying overnight. For comparison, samples with different cobalt acetate contents (50 mg and 200 mg) were also synthesized (labeled as Co<sub>2</sub>P/NPG-2 and Co<sub>2</sub>P/NPG-3).

**Electrochemical measurements:** All electrochemical experiments were performed on the CHI760E electrochemical workstation. Specifically, Co<sub>2</sub>P/NPG was used as the working electrode; a Ag/AgCl electrode and a graphite rod were used as the reference electrode and the counter electrode, respectively. In 0.5 M H<sub>2</sub>SO<sub>4</sub>, the linear scanning voltammetry curve was recorded at a scanning speed of 5 mV s<sup>-1</sup>. Electrochemical stability measurements were performed via 1000 CV cycles.

## 3. Results and Discussion

The fabrication process of Co<sub>2</sub>P/NPG is shown in Figure 1. Firstly, DNA-modified GO (DNA-GO) is coupled through the  $\pi$ - $\pi$  stacking between DNA and GO. Negatively charged phosphate groups on DNA could provide binding sites for Co<sup>2+</sup>. During the preparation process, the Co<sup>2+</sup> can bind to the DNA-GO due to the strong electrostatic interaction between the metal cations and the negatively charged phosphate groups on DNA. After a hydrothermal reaction, Co<sub>3</sub>O<sub>4</sub>/DNA-GO was obtained. Sufficient N and P elements in DNA enable the fabrication of Co<sub>2</sub>P and NPG without the need for an additional N and P source. Therefore, after carbonization, a Co<sub>2</sub>P/NPG composite is fabricated.

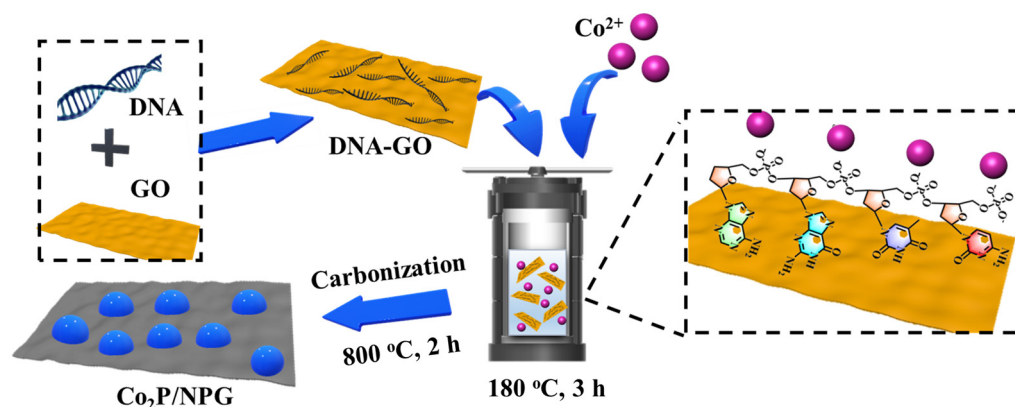


**Figure 1.** Schematic illustration of the synthesis of the  $\text{Co}_2\text{P}/\text{NPG}$  composite.

X-ray powder diffraction (XRD) was utilized to analyze the crystalline structure of the synthesized  $\text{Co}_2\text{P}$ . As depicted in Figure 2, the red vertical line is the standard card for  $\text{Co}_2\text{P}$  (PDF#32-0306). The XRD pattern showed five characteristic peaks located at  $40.7^\circ$ ,  $41^\circ$ ,  $43.3^\circ$ ,  $44.1^\circ$ ,  $51.5^\circ$ , and  $52^\circ$ , corresponding to the (121), (201), (211), (130), (131), and (002) crystal planes of  $\text{Co}_2\text{P}$ , respectively. There are no peaks of metallic cobalt, cobalt oxide, or other forms of cobalt phosphide ( $\text{CoP}$ ,  $\text{CoP}_2$ , etc.), thus proving the high purity of our product. The control sample of  $\text{Co}_2\text{P}$  was also detected via XRD, as shown in Figure S2, confirming the successful preparation of  $\text{Co}_2\text{P}$ .

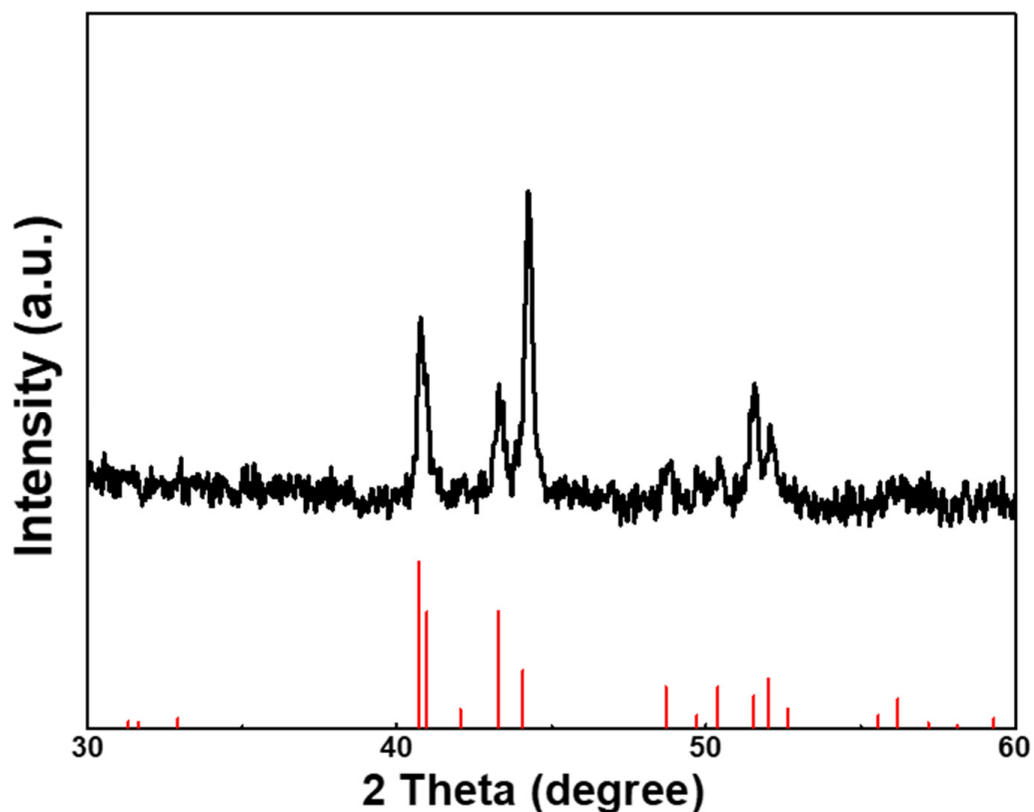


**Figure 2.** XRD pattern of  $\text{Co}_2\text{P}/\text{NPG}$ . The vertical lines at the base of the XRD pattern represent the standard diffractions of  $\text{Co}_2\text{P}$ .

Transmission electron microscopy (TEM) was utilized to detect the morphology of the as-prepared  $\text{Co}_2\text{P}/\text{NPG}$ . As clearly shown in Figure 3a, the  $\text{Co}_2\text{P}$  nanoparticles are uniformly dispersed on the graphene sheet. The high-resolution TEM (HRTEM) image of

Co<sub>2</sub>P nanoparticles (Figure 3b) presents clear lattice planes of 0.22 nm, which corresponded to the (121) plane of Co<sub>2</sub>P [20–22]. It is worth noting that the sample underwent long-term ultrasonication during the preparation process of the TEM sample, but no free cobalt phosphide particles were found during the testing process, thus proving the close binding between cobalt phosphide and N, P co-doped graphene. The energy-dispersive X-ray spectrum (EDS) results shown in Figure 3c in the region further illustrate the presence of C, N, O, Co, and P elements. The atomic ratio of Co and P derived from the EDS result was approximately 1.4:1, which is lower than the stoichiometric ratio of Co<sub>2</sub>P, indicating the successful doping of P onto the graphene sheet. In order to further verify the distribution of C, N, Co, and P elements in the composite, HAADF-STEM element mapping analysis was employed. Figure 3d is a STEM image of Co<sub>2</sub>P/NPG, and the distribution of C, N, Co, and P elements was analyzed based on this. As shown in Figure 3e,f, it can be found that the distribution of N and C elements is consistent, indicating that nitrogen was successfully doped onto graphene. The distribution of Co and P elements (Figure 3g,h) on the particles is basically consistent, which proves the successful preparation of cobalt phosphide nanoparticles.

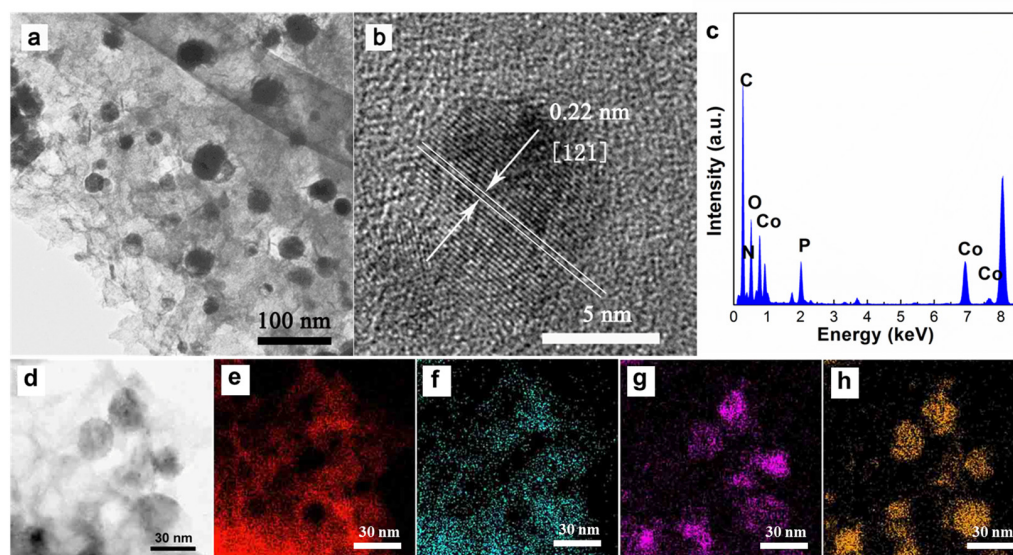


**Figure 3.** TEM (a) and HRTEM (b) images of Co<sub>2</sub>P/NPG. (c) EDS spectrum of Co<sub>2</sub>P/NPG. HAADF-STEM (d) image and the corresponding EDS mappings of C (e), N (f), Co (g), and P (h) elements for Co<sub>2</sub>P/NPG.

The surface elemental composition and chemical states of Co<sub>2</sub>P/NPG were detected through using X-ray photoelectron spectroscopy (XPS) characterization technology. Firstly, the chemical states of the elements for N, P co-doped carbon (NPC), which was synthesized via the carbonization of DNA, were detected through XPS. The results shown in Figure S1 confirm the successful preparation of NPC. As displayed in Figure 4a, the peaks can be divided into four peaks at 284.7, 286, 287.1, and 289.3 eV, contributing to the C-C, C-P, C-N, and C-O, respectively. The high-resolution spectrum of N 1s (Figure 4b) can be deconvoluted into two peaks, which can be ascribed to pyridinic N (398.2 eV) and graphitic N (400.6 eV), indicating the successful doping of N to the graphene sheet [23]. Figure 4c is the high-resolution spectrum of Co 2p, in which two peaks at 778.3 and 793.4 eV can be ascribed to Co 2p<sub>1/2</sub> and 2p<sub>3/2</sub> in Co<sub>2</sub>P [24]. The peaks at 781.2 and 797.2 eV may be due to the oxidation of cobalt ions on the surface of cobalt phosphide. The peaks at 786.0 and 802.9 eV are the satellite peaks, which can be found in transition metal-based materials. Figure 4d shows the high-resolution pattern of P 2p, which can be deconvoluted into four peaks: the two peaks at 129.5 and 130.3 eV corresponding to the P 2p<sub>3/2</sub> and P 2p<sub>1/2</sub> in Co<sub>2</sub>P, and the other two peaks located at 132.3 and 133.2 eV can be ascribed to P-C and P-O species [24,25]. The appearance of the P-C bond indicated the successful

doping of phosphorus onto the graphene sheet. The peak of the P-O bond is due to the surface oxidation of Co<sub>2</sub>P after air exposure. It should be noted that the P 2p<sub>3/2</sub> shows a negative shift of 0.6 eV compared with the elemental P (130.1 eV) [26]. While, compared with the energy level of the zero valent state of the metal cobalt (778 eV) [23], the binding energy of Co 2p<sub>1/2</sub> in the composite shows a slightly positive shift of 0.3 eV, indicating the transfer of electrons from cobalt to P. All of the above characterizations imply the successful fabrication of Co<sub>2</sub>P/NPG.

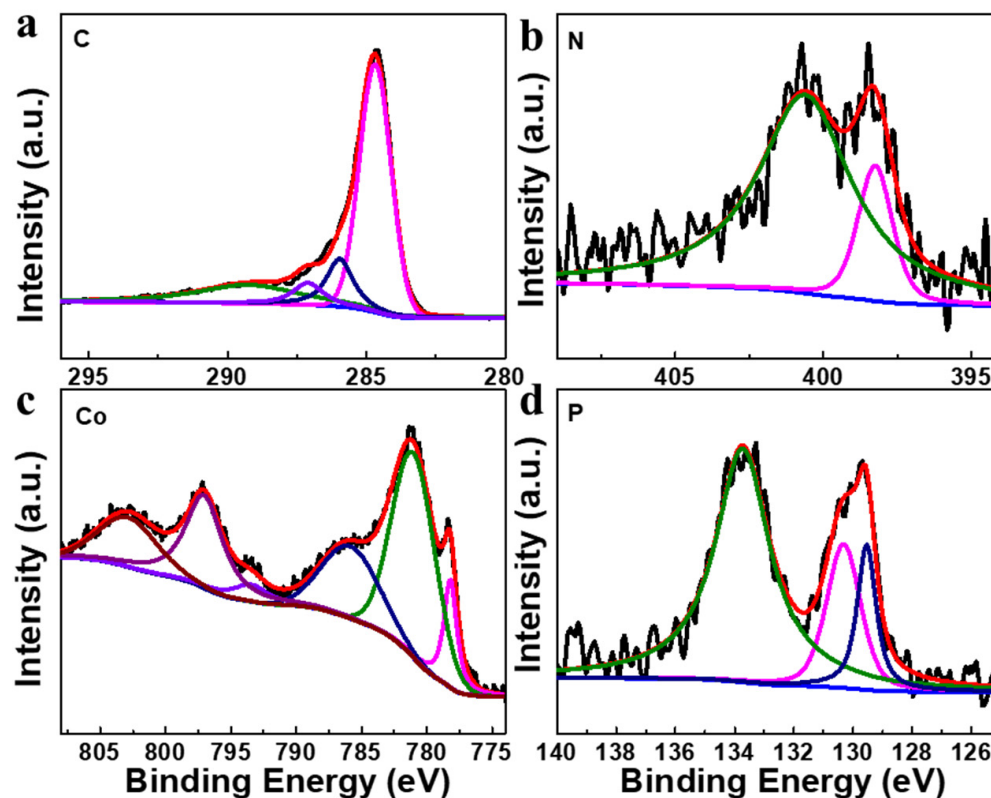


**Figure 4.** High-resolution XPS spectra of C 1s (a), N 1s (b), P 2p (c), and Co 2p (d) for Co<sub>2</sub>P/NPG.

Hydrogen evolution reaction activity was detected through using linear sweep voltammetry (LSV) with a scan rate of 5 mV s<sup>-1</sup> in 0.5 M H<sub>2</sub>SO<sub>4</sub>. For comparison, commercial Pt/C (20%), Co<sub>2</sub>P, and NPG were also detected. As depicted in Figure 5a, the commercial Pt/C (20%) shows the best activity, with an overpotential of 34 mV, yielding a current density of 10 mA cm<sup>-2</sup>. The obtained Co<sub>2</sub>P/NPG exhibits an overpotential of 144 mV, which is much lower than that of Co<sub>2</sub>P (266 mV) and NPG (467 mV). The Co<sub>2</sub>P/NPG exhibits superior activity than many of the recently reported non-noble metal electrocatalysts listed in Table S1. In order to optimize the synthetic conditions, catalysts with different contents of cobalt acetate (50 mg and 200 mg) were also synthesized (labeled as Co<sub>2</sub>P/NPG-2 and Co<sub>2</sub>P/NPG-3). As shown in Figure S3, Co<sub>2</sub>P/NPG shows the best activity with the lowest overpotential. In addition, the HER reaction kinetic activities were estimated via Tafel slope (Figure 5b). The Tafel slope of Co<sub>2</sub>P/NPG is about 72 mV dec<sup>-1</sup>, indicating that the reaction kinetics of Co<sub>2</sub>P/NPG follows the Volmer–Heyrovsky mechanism. For comparison, the Tafel slope of the 20% Pt/C was also tested (29 mV dec<sup>-1</sup>), which is consistent with the results reported in previous publications [27,28]. It can be observed that the Tafel slope for Co<sub>2</sub>P/NPG is drastically lower than that of Co<sub>2</sub>P (114 mV dec<sup>-1</sup>) and NPG (196 mV dec<sup>-1</sup>). A lower Tafel slope typically suggests more favorable HER kinetics, further demonstrating the synergistic contribution of the Co<sub>2</sub>P and NPG.

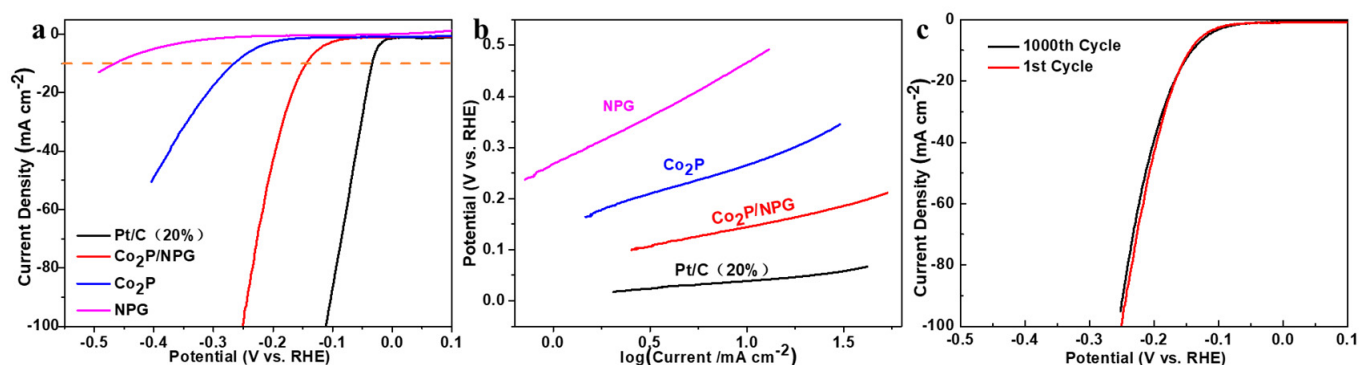


**Figure 5.** LSV curves (a) and corresponding Tafel plots (b) of Co<sub>2</sub>P/NPG, commercial Pt/C, Co<sub>2</sub>P, and NPG. (c) LSV curves of the Co<sub>2</sub>P/NPG before and after 1000 CV cycles.

Electrocatalytic stability is a key factor for evaluating the performance of the electrocatalysts, especially for further utilization in practical applications. Continuous cyclic voltammetry (CV) sweeps were conducted at a sweep rate of 100 mV s<sup>-1</sup>. As shown in Figure 5c, after continuous detection for 1000 cycles, the polarization curves were almost consistent with the initial test, indicating the excellent stability of Co<sub>2</sub>P/NPG. Moreover, a TEM image of the Co<sub>2</sub>P/NPG after the stability test was also test. As shown in Figure S4, after the stability test, the morphology of the sample does not show obvious changes, and the nanoparticles are evenly dispersed on the graphene sheet, further confirming the stability of the catalysts.

#### 4. Conclusions

In summary, a green strategy for the preparation of N, P co-doped graphene-supported Co<sub>2</sub>P nanoparticles has been proposed in this study. In this strategy, the purpose of DNA is three-fold: (1) providing loading sites for catching Co<sup>2+</sup>; (2) acting as a green phosphorus source for the preparation of Co<sub>2</sub>P; and (3) acting as a N and P source for N, P doping in graphene. Due to the synergistic effect of NPG and Co<sub>2</sub>P, the as-prepared Co<sub>2</sub>P/NPG exhibits high activity, with a low overpotential (144 mV) and a small Tafel slope (72 mV dec<sup>-1</sup>). This study provides a successful green synthesis strategy for the preparation of high-performance TMPs.

**Supplementary Materials:** The following supporting information can be downloaded at: <https://www.mdpi.com/article/10.3390/ma16186119/s1>, Figure S1: High-resolution XPS spectra of C 1s (a), N 1s (b) and P 2p (c) for NPC; Table S1: The comparison of the catalytic performance with other non-noble metal catalysts [7,29–36]; Figure S2: XRD pattern of Co<sub>2</sub>P; Figure S3: LSV curves of Co<sub>2</sub>P/NPG synthesized with different contents of cobalt; Figure S4: TEM image of Co<sub>2</sub>P/NPG after stability test.

**Author Contributions:** Conceptualization, J.M. and J.W.; methodology, J.M.; software, J.L.; validation, J.L. and Y.T.; formal analysis, T.Z.; investigation, J.M.; resources, J.M.; writing—original draft preparation, J.M.; writing—review and editing, J.W.; visualization, J.M. and J.L.; funding acquisition, J.M. All authors have read and agreed to the published version of the manuscript.

**Funding:** This research was funded by the Fundamental Research Funds for the Central Universities (No. 2022XJHH02).

**Institutional Review Board Statement:** Not applicable.

**Conflicts of Interest:** The authors declare no conflict of interest.

#### References

1. El-Refaei, S.M.; Russo, P.A.; Pinna, N. Recent Advances in Multimetal and Doped Transition-Metal Phosphides for the Hydrogen Evolution Reaction at Different pH values. *ACS Appl. Mater. Interfaces* **2021**, *13*, 22077–22097. [CrossRef]
2. Zhu, Y.; Lin, Q.; Zhong, Y.; Tahini, H.A.; Shao, Z.; Wang, H. Metal oxide-based materials as an emerging family of hydrogen evolution electrocatalysts. *Energy Environ. Sci.* **2020**, *13*, 3361–3392. [CrossRef]

3. Zhu, J.; Hu, L.; Zhao, P.; Lee, L.Y.S.; Wong, K.Y. Recent Advances in Electrocatalytic Hydrogen Evolution Using Nanoparticles. *Chem. Rev.* **2020**, *120*, 851–918. [[CrossRef](#)] [[PubMed](#)]
4. Zhang, N.; Li, Y.; Zhang, R.; Huang, S.; Wang, F.; Tang, M.; Liu, J. Tiny Ni<sub>3</sub>S<sub>2</sub> boosting MoS<sub>2</sub> hydrogen evolution in alkali by enlarging coupling boundaries and stimulating basal plane. *J. Colloid Interface Sci.* **2023**, *642*, 479–487. [[CrossRef](#)] [[PubMed](#)]
5. Bai, X.; Cao, T.; Xia, T.; Wu, C.; Feng, M.; Li, X.; Mei, Z.; Gao, H.; Huo, D.; Ren, X.; et al. MoS<sub>2</sub>/NiSe<sub>2</sub>/rGO Multiple-Interfaced Sandwich-like Nanostructures as Efficient Electrocatalysts for Overall Water Splitting. *Nanomaterials* **2023**, *13*, 752. [[CrossRef](#)] [[PubMed](#)]
6. Zhu, J.; Du, Q.; Khan, M.A.; Zhao, H.; Fang, J.; Ye, D.; Zhang, J. 2D porous Co-Mo nitride heterostructures nanosheets for highly effective electrochemical water splitting. *Appl. Surf. Sci.* **2023**, *623*, 156989. [[CrossRef](#)]
7. Chang, H.; Liang, Z.; Lang, K.; Fan, J.; Ji, L.; Yang, K.; Lu, S.; Ma, Z.; Wang, L.; Wang, C. Pencil-like Hollow Carbon Nanotubes Embedded CoP-V<sub>4</sub>P<sub>3</sub> Heterostructures as a Bifunctional Catalyst for Electrocatalytic Overall Water Splitting. *Nanomaterials* **2023**, *13*, 1667. [[CrossRef](#)]
8. Ma, J.; Wang, M.; Lei, G.; Zhang, G.; Zhang, F.; Peng, W.; Fan, X.; Li, Y. Polyaniline Derived N-Doped Carbon-Coated Cobalt Phosphide Nanoparticles Deposited on N-Doped Graphene as an Efficient Electrocatalyst for Hydrogen Evolution Reaction. *Small* **2018**, *14*, 1702895. [[CrossRef](#)]
9. Li, P.; Li, W.; Zhao, S.; Huang, Y.; Tian, S.; Huang, X. Advanced hydrogen evolution electrocatalysis enabled by ruthenium phosphide with tailored hydrogen binding strength via interfacial electronic interaction. *Chem. Eng. J.* **2022**, *429*, 132557. [[CrossRef](#)]
10. Vijayakuma, E.; Ramakrishnan, S.; Sathiskumar, C.; Yoo, D.J.; Balamurugan, J.; Noh, H.S.; Kwon, D.; Kim, Y.H.; Lee, H. MOF-derived CoP-nitrogen-doped carbon@NiFeP nanoflakes as an efficient and durable electrocatalyst with multiple catalytically active sites for OER, HER, ORR and rechargeable zinc-air batteries. *Chem. Eng. J.* **2022**, *428*, 131115. [[CrossRef](#)]
11. Yuan, W.; Jiang, T.; Fang, X.; Fan, Y.; Qian, S.; Gao, Y.; Cheng, N.; Xue, H.; Tian, J. Interface engineering of S-doped Co<sub>2</sub>P@Ni<sub>2</sub>P core-shell heterostructures for efficient and energy-saving water splitting. *Chem. Eng. J.* **2022**, *439*, 135743. [[CrossRef](#)]
12. Li, J.; Chen, C.; Lv, Z.; Ma, W.; Wang, M.; Li, Q.; Dang, J. Constructing heterostructures of ZIF-67 derived C, N doped Co<sub>2</sub>P and Ti<sub>2</sub>VC<sub>2</sub>T<sub>x</sub>MXene for enhanced OER. *J. Mater. Sci. Technol.* **2023**, *145*, 74–82. [[CrossRef](#)]
13. Zhao, X.; Levell, Z.H.; Yu, S.; Liu, Y. Atomistic Understanding of Two-dimensional Electrocatalysts from First Principles. *Chem. Rev.* **2022**, *122*, 10675–10709. [[PubMed](#)]
14. Tsounis, C.; Subhash, B.; Kumar, P.V.; Bedford, N.M.; Zhao, Y.; Shenoy, J.; Ma, Z.; Zhang, D.; Toe, C.Y.; Cheong, S.; et al. Pt Single Atom Electrocatalysts at Graphene Edges for Efficient Alkaline Hydrogen Evolution. *Adv. Funct. Mater.* **2022**, *32*, 2203067. [[CrossRef](#)]
15. Feng, D.; Dong, Y.; Nie, P.; Zhang, L.; Qiao, Z.-A. CoNiCuMgZn high entropy alloy nanoparticles embedded onto graphene sheets via anchoring and alloying strategy as efficient electrocatalysts for hydrogen evolution reaction. *Chem. Eng. J.* **2022**, *430*, 132883. [[CrossRef](#)]
16. Zheng, Y.; Jiao, Y.; Li, L.H.; Xing, T.; Chen, Y.; Jaroniec, M.; Qiao, S.Z. Toward Design of Synergistically Active Carbon-Based Catalysts for Electrocatalytic Hydrogen Evolution. *ACS Nano* **2014**, *8*, 5290–5296. [[CrossRef](#)] [[PubMed](#)]
17. Chen, Z.; Liu, C.; Cao, F.; Ren, J.; Qu, X. DNA metallization: Principles, methods, structures, and applications. *Chem. Soc. Rev.* **2018**, *47*, 4017–4072.
18. Wang, H.; Bo, X.; Luhana, C.; Guo, L. Nitrogen doped large mesoporous carbon for oxygen reduction electrocatalyst using DNA as carbon and nitrogen precursor. *Electrochem. Commun.* **2012**, *21*, 5–8. [[CrossRef](#)]
19. Ma, J.; Li, X.; Lei, G.; Wang, J.; Wang, J.; Liu, J.; Ke, M.; Li, Y.; Sun, C. A general synthetic strategy for N, P co-doped graphene supported metal-rich noble metal phosphides for hydrogen generation. *Green Energy Environ.* **2022**. [[CrossRef](#)]
20. Qin, M.; Chen, L.; Zhang, H.; Humayun, M.; Fu, Y.; Xu, X.; Xue, X.; Wang, C. Achieving highly efficient pH-universal hydrogen evolution by Mott-Schottky heterojunction of Co<sub>2</sub>P/Co<sub>4</sub>N. *Chem. Eng. J.* **2023**, *454*, 140230. [[CrossRef](#)]
21. Huang, G.; Hu, M.; Xu, X.; Alothman, A.A.; Mushab, M.S.S.; Ma, S.; Shen, P.K.; Zhu, J.; Yamauchi, Y. Optimizing Heterointerface of Co<sub>2</sub>P-Co<sub>x</sub>O<sub>y</sub> Nanoparticles within a Porous Carbon Network for Deciphering Superior Water Splitting. *Small Struct.* **2023**, *4*, 2200235. [[CrossRef](#)]
22. Guo, R.; Shi, J.; Hong, L.; Ma, K.; Zhu, W.; Yang, H.; Wang, J.; Wang, H.; Sheng, M. CoP<sub>2</sub>/Co<sub>2</sub>P Encapsulated in Carbon Nanotube Arrays to Construct Self-Supported Electrodes for Overall Electrochemical Water Splitting. *ACS Appl. Mater. Interfaces* **2022**, *14*, 56847–56855. [[CrossRef](#)]
23. Xie, H.; Zeng, D.; Du, B.; Zhang, P.; Lin, H.; Li, Q.; Lin, Z.; Li, W.; Meng, Y. Co<sub>2</sub>P encapsulated in N, O co-doped carbons as bifunctional electrocatalysts for oxygen evolution and reduction reactions. *Int. J. Hydrogen Energy* **2023**, *48*, 9273–9284. [[CrossRef](#)]
24. Zhang, Y.; Shi, W.; Bo, L.; Shen, Y.; Ji, X.; Xia, L.; Guan, X.; Wang, Y.; Tong, J. Electrospinning construction of heterostructural Co<sub>3</sub>W<sub>3</sub>C/CoP nanoparticles embedded in N, P-doped hierarchically porous carbon fibers as excellent multifunctional electrocatalyst for Zn-air batteries and water splitting. *Chem. Eng. J.* **2022**, *431*, 134188. [[CrossRef](#)]
25. Zhao, Q.; Ge, Y.; Wang, X. Metal-organic-framework-derived cubic Co<sub>2</sub>P@NC for fast sodium-ion storage. *J. Alloys Compd.* **2023**, *947*, 169346. [[CrossRef](#)]
26. Li, J.-S.; Huang, M.-J.; Zhou, Y.-W.; Chen, X.-N.; Yang, S.; Zhu, J.-Y.; Liu, G.-D.; Ma, L.-J.; Cai, S.-H.; Han, J.-Y. RuP<sub>2</sub>-based hybrids derived from MOFs: Highly efficient pH-universal electrocatalysts for the hydrogen evolution reaction. *J. Mater. Chem. A* **2021**, *9*, 12276–12282. [[CrossRef](#)]

27. Da, Y.; Jiang, R.; Tian, Z.; Chen, G.; Xiao, Y.; Zhang, J.; Xi, S.; Deng, Y.; Chen, W.; Han, X.; et al. Development of a Novel Pt<sub>3</sub>V Alloy Electrocatalyst for Highly Efficient and Durable Industrial Hydrogen Evolution Reaction in Acid Environment. *Adv. Energy Mater.* **2023**, *13*, 2300127. [[CrossRef](#)]
28. Hsiao, C.-Y.; Dang, V.D.; Hsu, Y.-W.; Lu, Y.-T.; Hsu, P.-J.; Le, P.A.; Wei, K.-H. Dual-cathode plasma-induced exfoliated WSe<sub>2</sub>/graphene nanosheet composite mediating an efficient hydrogen evolution reaction. *Electrochim. Acta* **2023**, *448*, 142169. [[CrossRef](#)]
29. Zou, L.; Wei, Y.S.; Wang, Q.; Liu, Z.; Xu, Q.; Kitagawa, S. Cobalt phosphide nanofibers derived from metal-organic framework composites for oxygen and hydrogen evolutions. *Sci. China Mater.* **2023**, *66*, 3139–3145. [[CrossRef](#)]
30. Yue, C.; Liu, N.; Li, Y.; Liu, Y.; Sun, F.; Bao, W.; Tuo, Y.; Pan, Y.; Jiang, P.; Zhou, Y.; et al. From atomic bonding to heterointerfaces: Co<sub>2</sub>P/WC constructed by lacunary polyoxometalates induced strategy as efficient hydrogen evolution electrocatalysts at all pH values. *J. Colloid Interface Sci.* **2023**, *645*, 276–286. [[CrossRef](#)]
31. Fang, B.; He, N.; Li, Y.; Lu, T.; He, P.; Chen, X.; Zhao, Z.; Pan, L. Prussian blue-derived hollow carbon-wrapped Fe-doped CoS<sub>2</sub> nanocages as durable electrocatalyst for efficient hydrogen evolution. *Electrochim. Acta* **2023**, *448*, 142187. [[CrossRef](#)]
32. Ning, S.; Wu, Q.; Zhu, Y.; Liu, S.; Zhou, W.; Mi, L.; Zhou, K.; Zhao, D.; Zhang, X.; Wang, N. N-doped carbon nanowire array confined cobalt phosphides as efficient bifunctional electrocatalysts for water splitting. *Inorg. Chem. Front.* **2023**, *10*, 2145–2153. [[CrossRef](#)]
33. Kurbanjan, D.; Li, X.; Du, H. B. N-co-doped and C-coated Co<sub>2</sub>P composite derived from phytate derivatives as a high-efficiency HER electrocatalyst. *CrystEngComm* **2023**, *25*, 2717–2727. [[CrossRef](#)]
34. Pan, Y.; Sun, K.; Liu, S.; Cao, X.; Wu, K.; Cheong, W.C.; Chen, Z.; Wang, Y.; Li, Y.; Liu, Y.; et al. Core-shell ZIF-8@ZIF-67-derived CoP nanoparticle-embedded N-doped carbon nanotube hollow polyhedron for efficient overall water splitting. *J. Am. Chem. Soc.* **2018**, *140*, 2610–2618. [[CrossRef](#)]
35. Zhang, X.Y.; Guo, B.Y.; Chen, Q.W.; Dong, B.; Zhang, J.Q.; Qin, J.F.; Xie, J.-Y.; Yang, M.; Wang, L.; Chai, Y.-M.; et al. Ultrafine and highly-dispersed bimetal Ni<sub>2</sub>P/Co<sub>2</sub>P encapsulated by hollow N-doped carbon nanospheres for efficient hydrogen evolution. *Int. J. Hydrogen Energy* **2019**, *44*, 14908–14917. [[CrossRef](#)]
36. Li, X.; Ma, J.; Luo, J.; Cheng, S.; Gong, H.; Liu, J.; Xu, C.; Zhao, Z.; Sun, Y.; Song, W.; et al. Porous N, P co-doped carbon-coated ultrafine Co<sub>2</sub>P nanoparticles derived from DNA: An electrocatalyst for highly efficient hydrogen evolution reaction. *Electrochim. Acta* **2021**, *393*, 139051. [[CrossRef](#)]

**Disclaimer/Publisher’s Note:** The statements, opinions and data contained in all publications are solely those of the individual author(s) and contributor(s) and not of MDPI and/or the editor(s). MDPI and/or the editor(s) disclaim responsibility for any injury to people or property resulting from any ideas, methods, instructions or products referred to in the content.